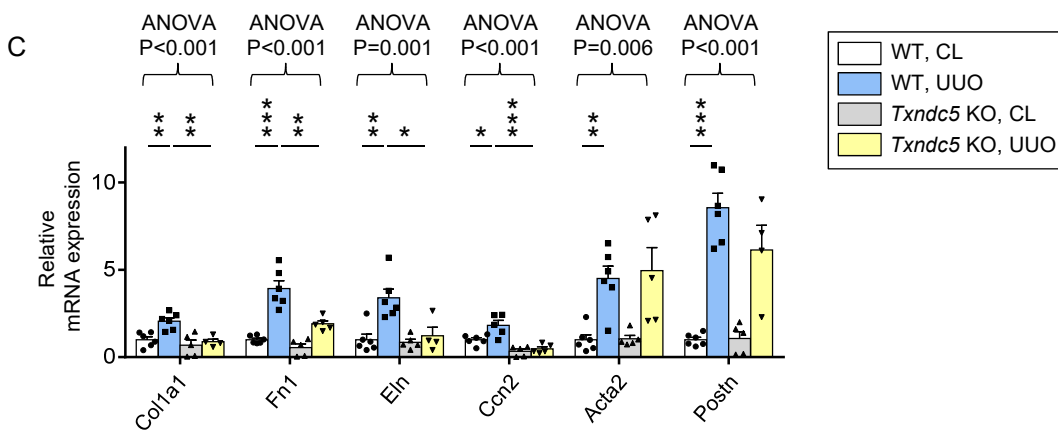
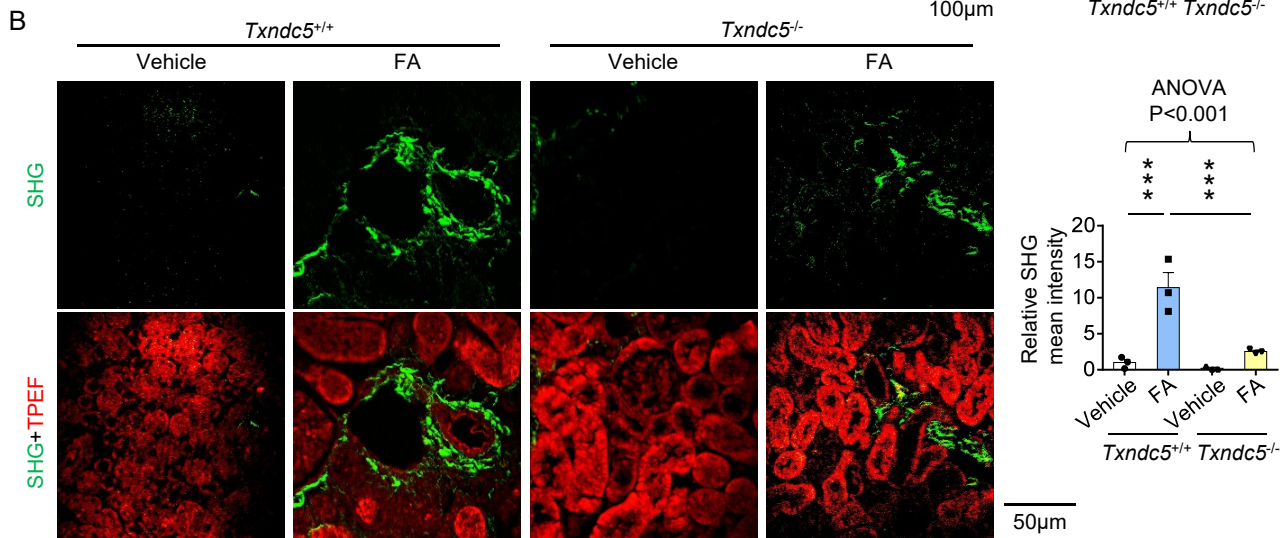
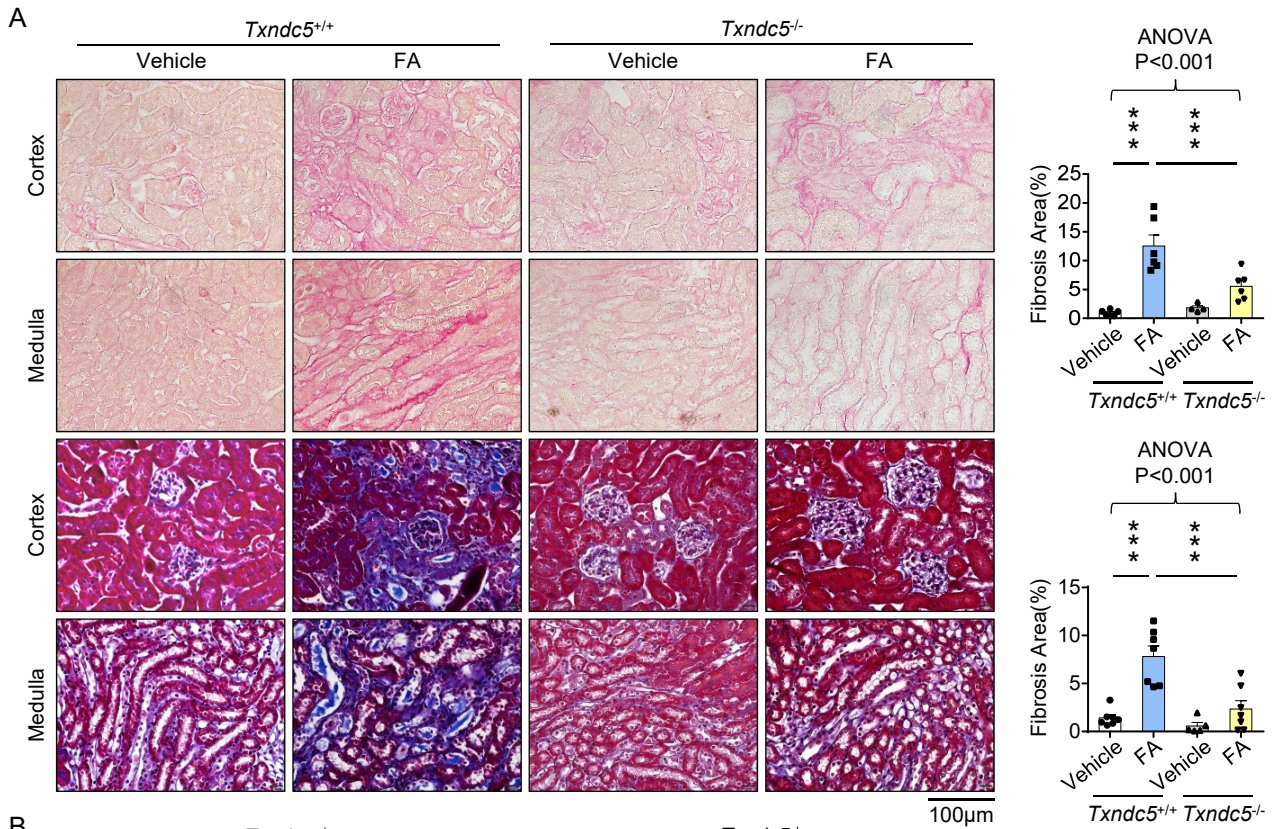
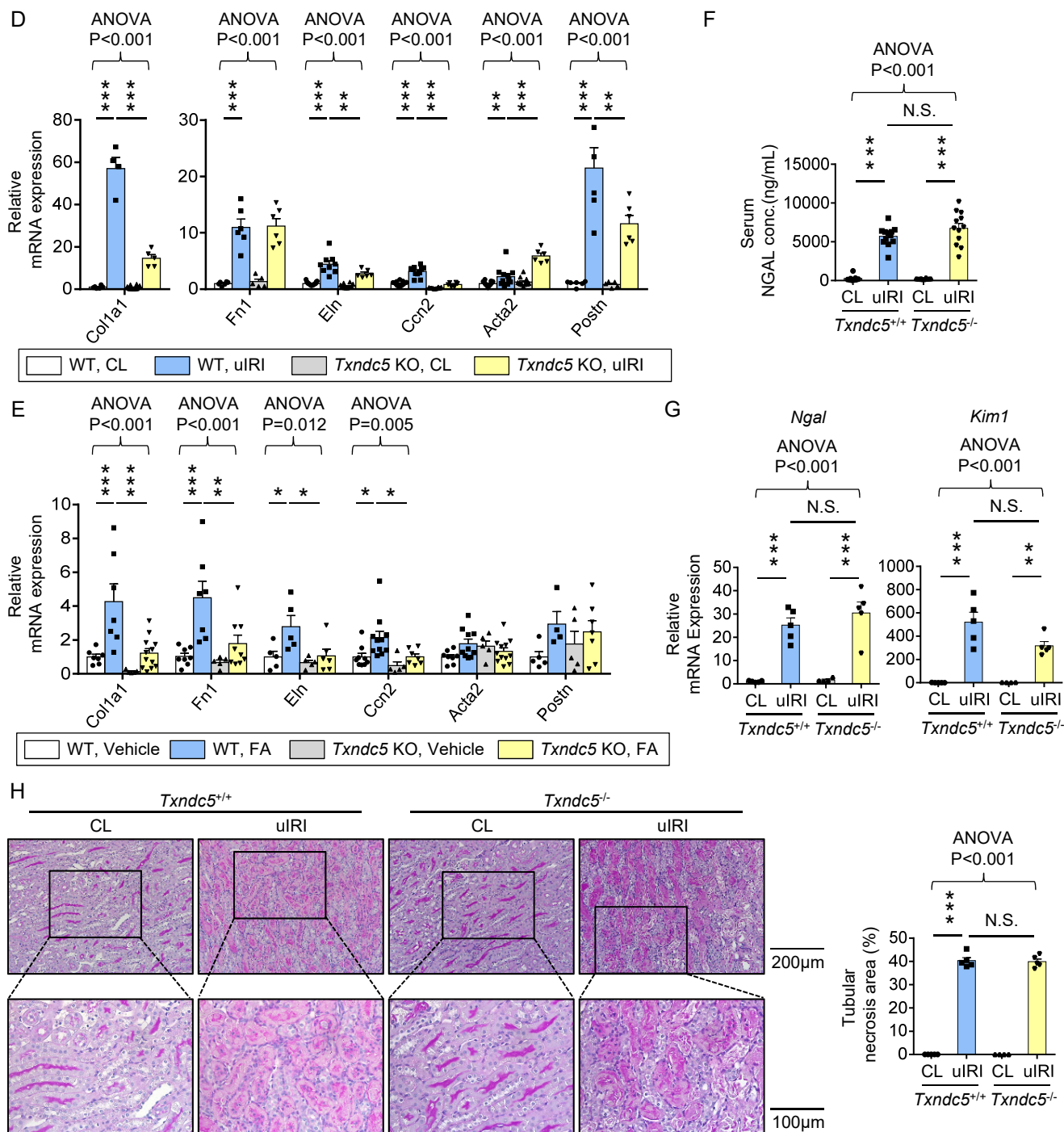
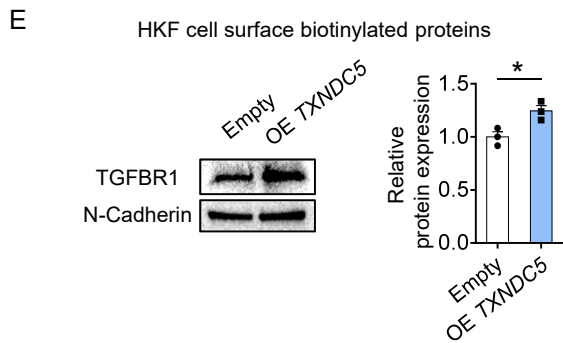
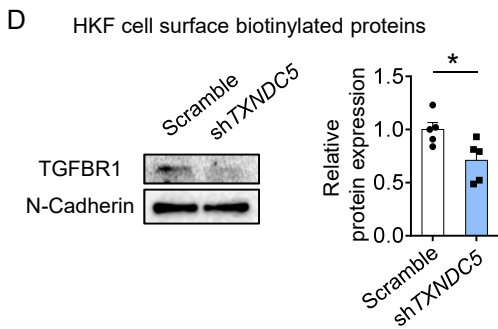
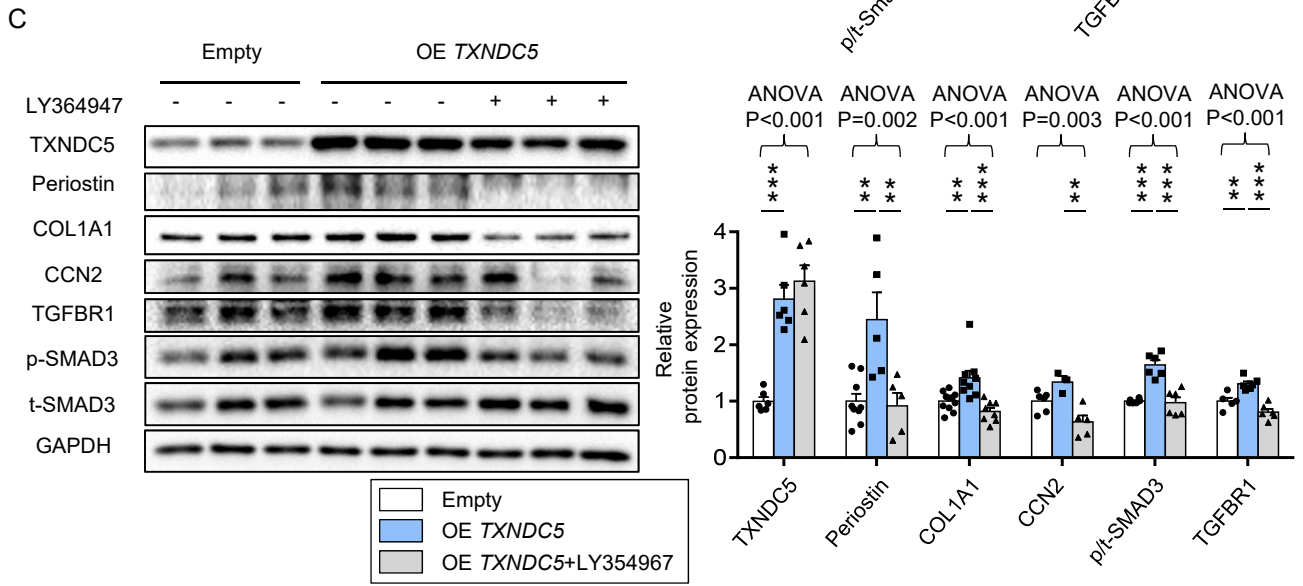
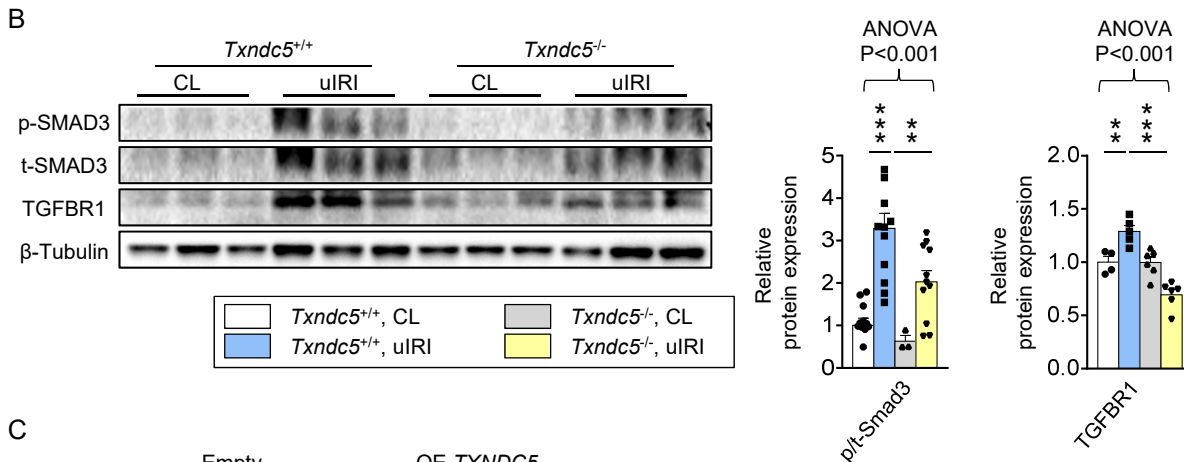
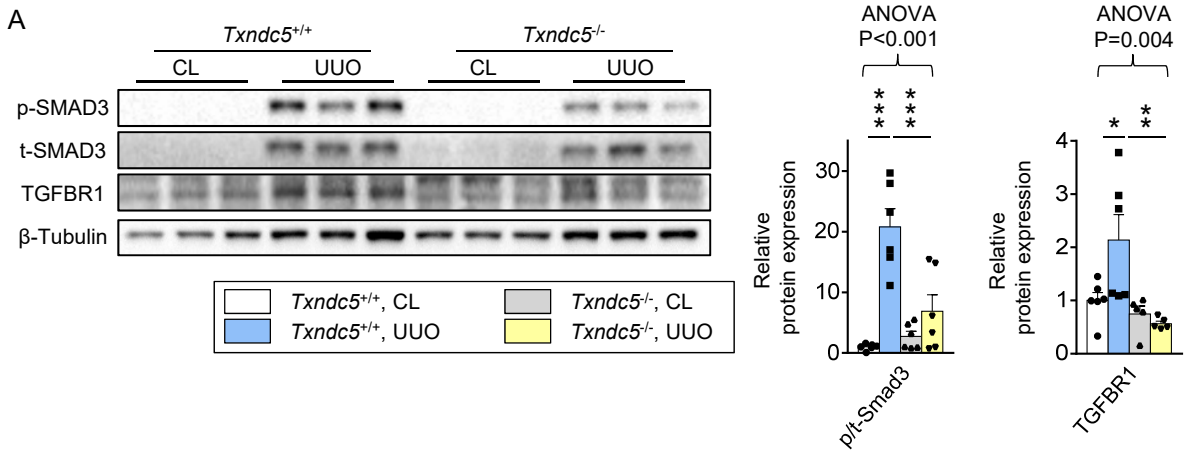


Supplementary Figure 2. TXNDC5 was highly upregulated in renal fibroblasts of the fibrotic kidneys. (A-B) IF staining of TXNDC5 (red) on sections of fibrotic kidneys induced by uIRI- (n=6) and FA- (n=3) in *Col1a1-GFP^{T9}* mice showed that TXNDC5 was mainly expressed in renal fibroblasts. Cell nuclei were stained with DAPI (blue). Scale bar: 100 µm. **(C)** Flow cytometry analysis of fibroblasts isolated from UUO-induced fibrotic mouse kidneys showed a marked expansion in TXNDC5⁺-kidney fibroblasts as well as a significant upregulation of TXNDC5 in these cells, compared to those from contralateral control kidneys. (n=496 and 1237, CL and UUO, respectively) Data are representative of three or more independent experimental replicates. For all panels, data were presented as mean ± SEM. *P<0.05, **P<0.01, ***P<0.001 by 2-sided t test

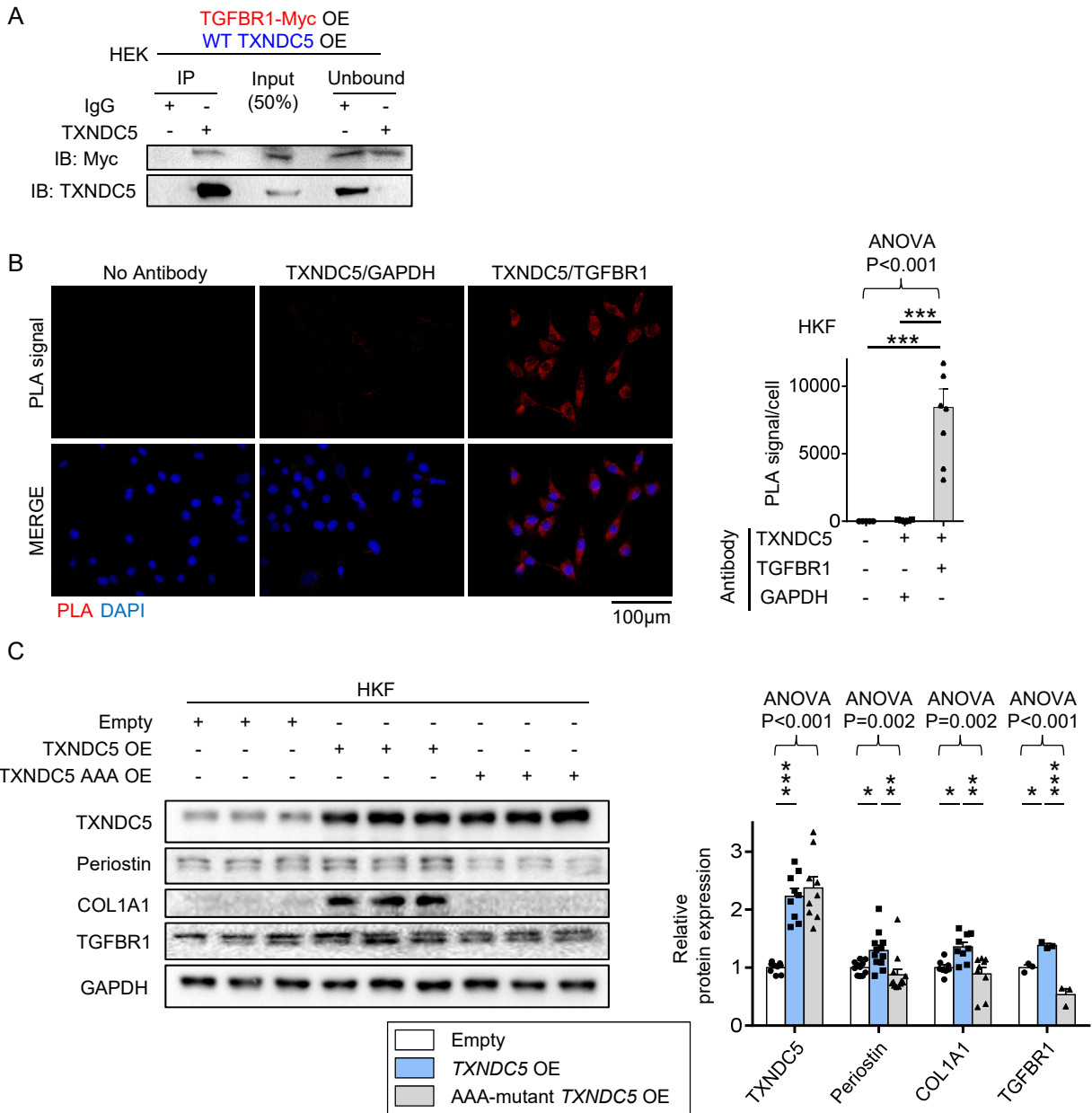




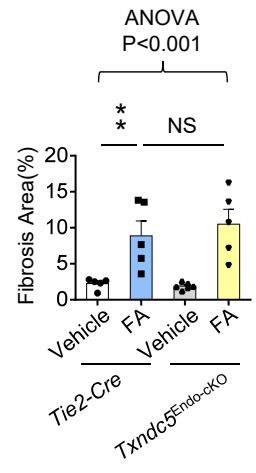
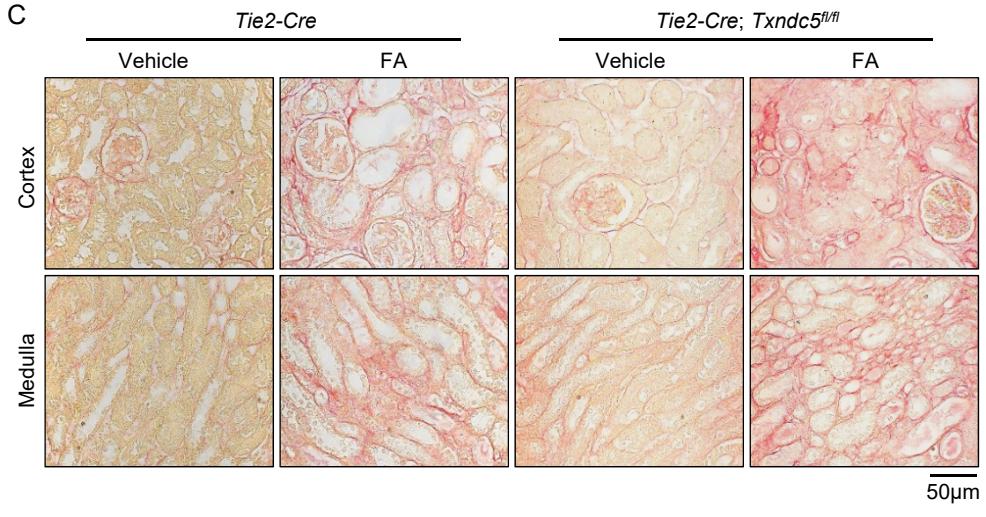
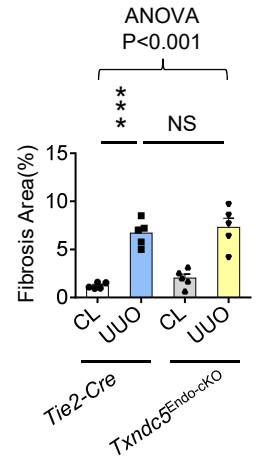
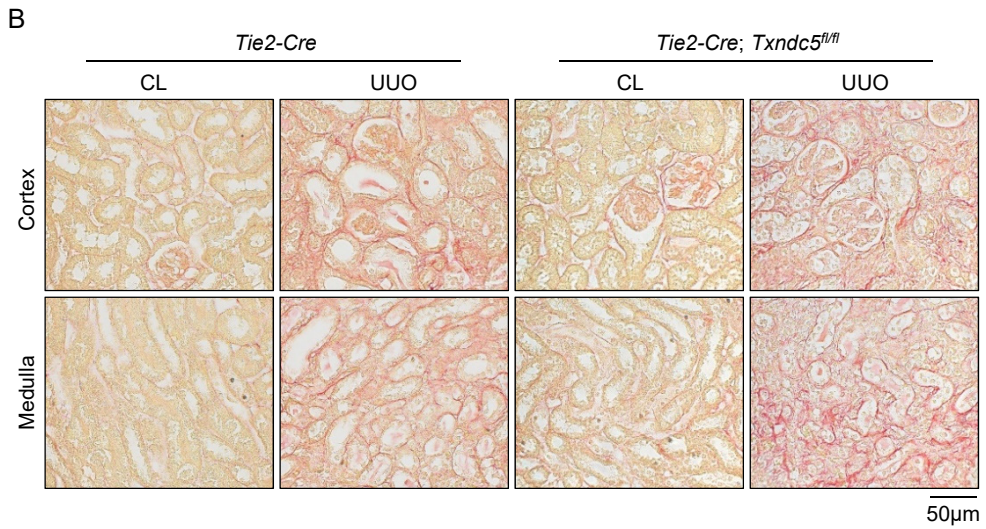
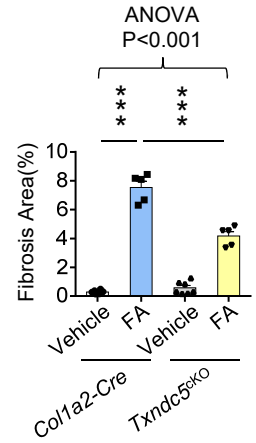
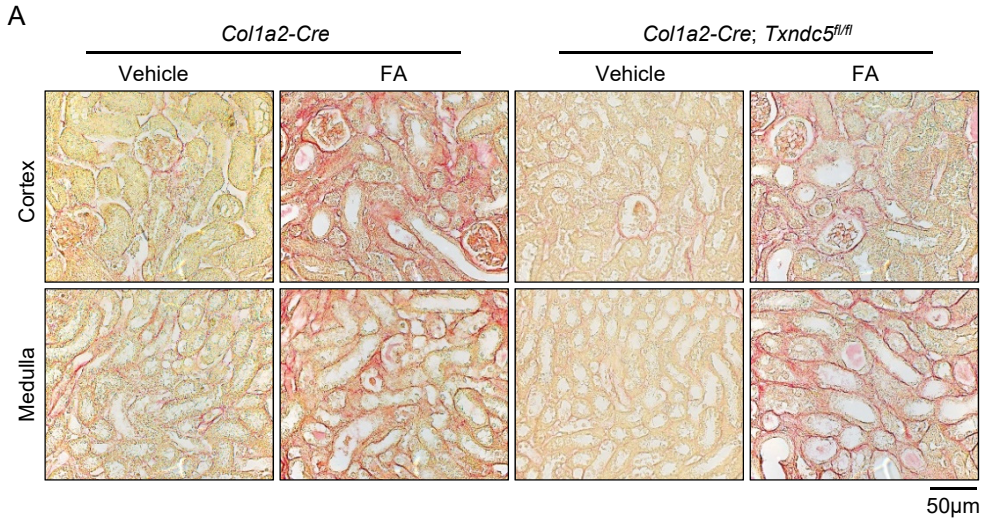
Supplementary Figure 3. *Txndc5* deletion attenuated renal fibrosis without affecting the extent of acute kidney injury (A) Picrosirius red staining (top two panels) and Masson's trichrome staining (bottom two panels) of kidney sections from WT and *Txndc5*^{-/-} mice 14 days after FA. Bar graphs of the quantitative results of Picrosirius red and Masson's trichrome staining were shown on the right. (n=5-7) Scale bar: 100 μ m. **(B)** Second harmonic generation (SHG) images of kidney sections from WT and *Txndc5*^{-/-} mice 14 days after FA. The quantitative results of SHG-positive areas showed accumulation of fibrillar collagen in WT, but not in *Txndc5*^{-/-} mouse kidneys following injury. (n=3) VE: vehicle. Scale bar: 50 μ m. **(C-E)** Transcript expression levels of fibroblast activation markers (*Postn* and *Acta2*) and ECM (*Col1a1*, *Fn1*, *Eln*, and *Ccn2*) quantified in the whole-kidney extracts from WT and *Txndc5*^{-/-} mice **(C)** 10 days after UUO, **(D)** 28 days after uIRI, or **(E)** 14 days after FA. (n=4-10) **(F)** Serum level of neutrophil gelatinase-associated lipocalin (NGAL) was elevated in WT mice one day after uIRI surgery and similarly increased in *Txndc5*^{-/-} mice. (n=9-18) **(G)** Transcript levels of *Ngal* and *Kim-1* were similarly increased in both WT and *Txndc5*^{-/-} kidneys one day after uIRI. (n=5) **(H)** PAS staining of kidney sections one day after uIRI did not show significant differences in the areas of tubular necrosis in WT and *Txndc5*^{-/-} mice. (n=5) Scale bar: 200 μ m (top panels), 100 μ m (bottom panels). Data are representative of three or more independent experimental replicates. For all panels, data were presented as mean \pm SEM. Statistical significance of differences among three or more groups was determined using one-way ANOVA, followed by Sidak's post hoc tests. *P<0.05, **P<0.01, ***P<0.001 by Sidak's multiple comparisons test.

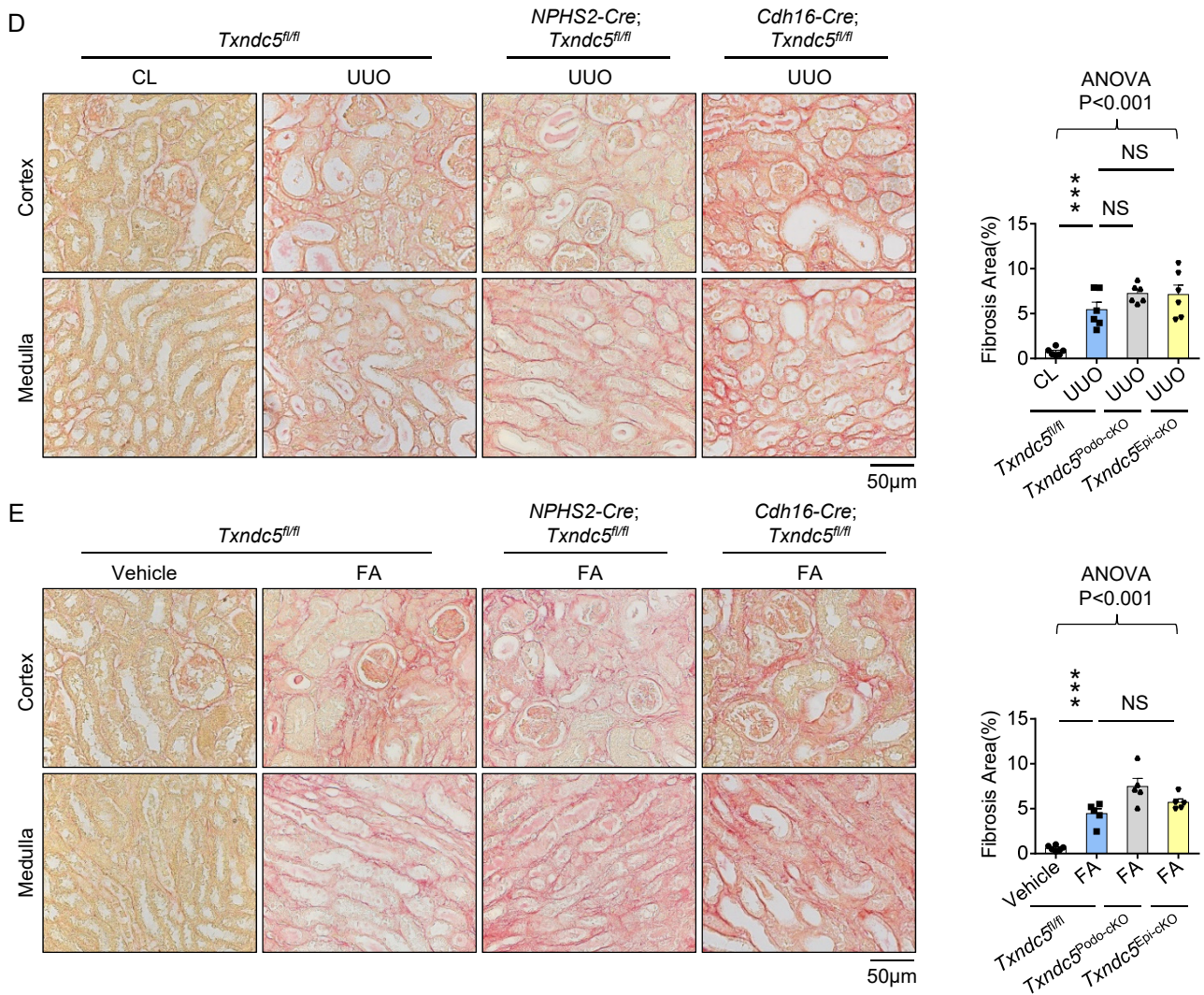


Supplementary Figure 4. TXNDC5-mediated fibrogenic responses are dependent on TGFBR1. (A-B) Global deletion of *Txndc5* attenuated upregulation of TGFBR1 and phosphorylation of SMAD3 in (A) UUC- or (B) uIRI-induced fibrotic kidney. (n=5-10) (C) Treatment of TGFBR1 inhibitor LY364947 (10 μ M) reduced the upregulation of fibroblast activation markers and ECM proteins induced by *TXNDC5* overexpression. (n=3-10) (D) Knockdown of *TXNDC5* decreased cell surface expression of TGFBR1 in HKF. (n=5) (E) Overexpression of *TXNDC5* increased cell surface expression of TGFBR1 in HKF. (n=3) For (D-E), cell surface TGFBR1 level was expressed relative to that of endogenous control membranous protein N-cadherin. Data are representative of three or more independent experimental replicates. For all panels, data were presented as mean \pm SEM. The statistical significance of differences among three or more groups was determined using one-way ANOVA, followed by Sidak's post hoc tests. *P<0.05, **P<0.01, ***P<0.001 by 2-sided t test (for two groups) or Sidak's multiple comparisons test (for three or more groups).

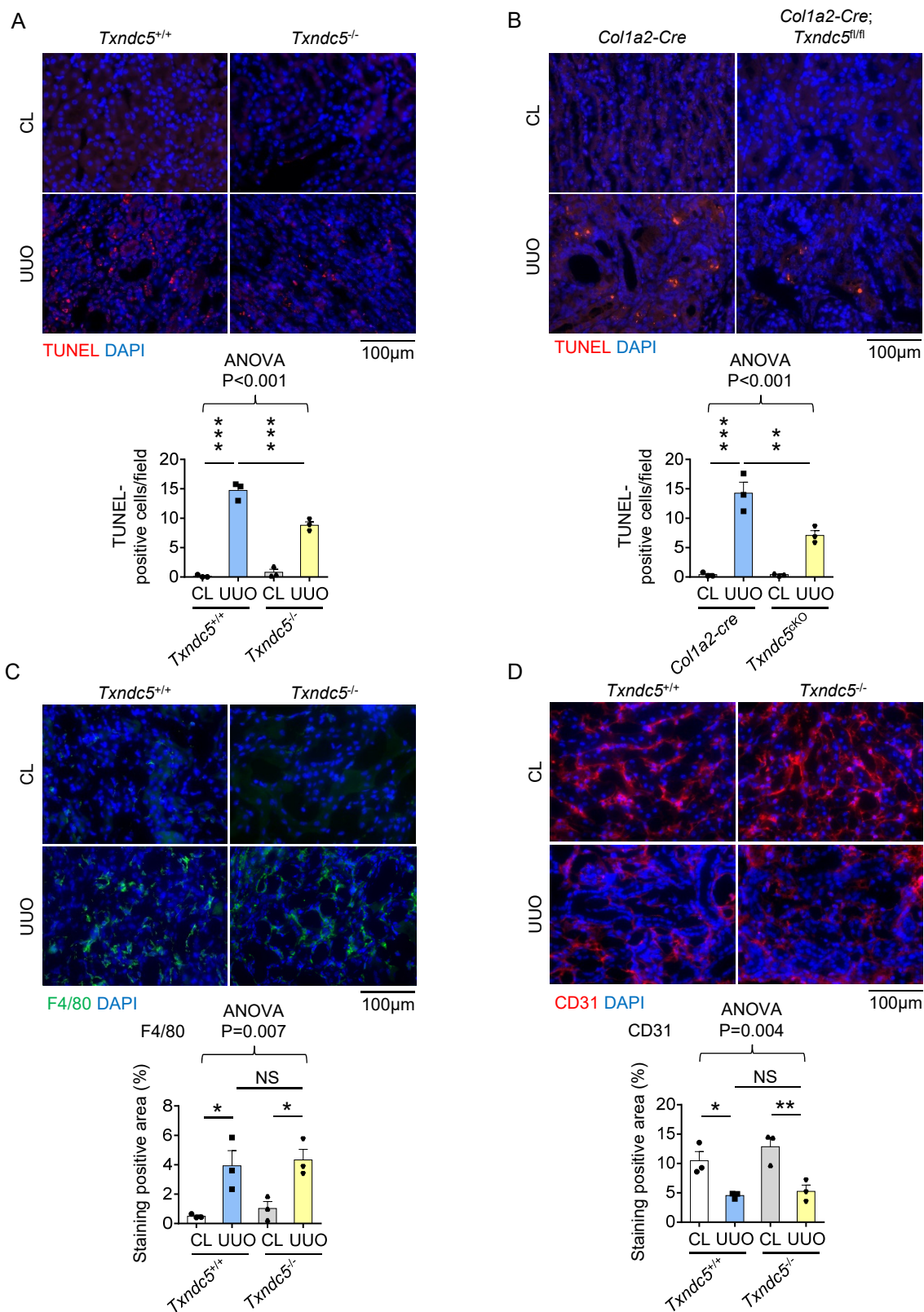


Supplementary Figure 5. TXNDC5 binds TGFBR1 and increases TGFBR1 level/fibrogenesis through its PDI activity. (A) Co-immunoprecipitation assay showed physical interaction between TXNDC5 and TGFBR1 (Myc-tagged). (B) Proximity Ligation Assay (PLA) showed increased PLA signals in HKF treated with antibodies specifically recognizing TXNDC5 and TGFBR1 compared with negative controls (TXNDC5 and GAPDH antibodies or without antibodies) (n=5-8) Scale bar: 100 µm. (C) Immunoblots showed that overexpression of WT, but not AAA-mutant, TXNDC5 in HKF induced the upregulation of TGFBR1, fibroblast activity markers, and ECM proteins. (n=3-12) Data are representative of three or more independent experimental replicates. For all panels, data were presented as mean ± SEM. The statistical significance of differences among three or more groups was determined using one-way ANOVA, followed by Sidak's post hoc tests. *P<0.05, **P<0.01, ***P<0.001 by Sidak's multiple comparisons test.



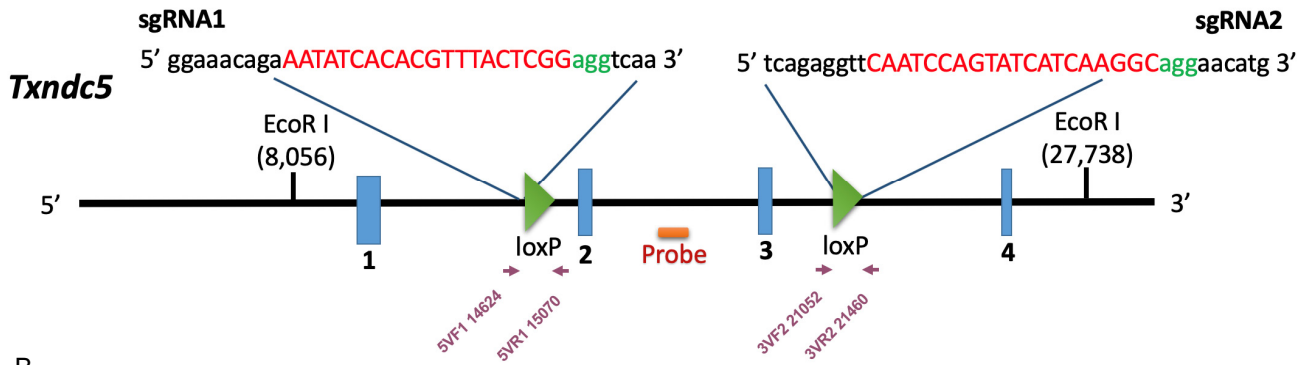


Supplementary Figure 6. Targeted deletion of *Txndc5* in renal fibroblasts, but not TECs, podocytes, or endothelial cells, attenuated kidney fibrosis. (A) Picosirius red staining of kidney sections from *Col1a2-Cre* and *Txndc5^{ckO}* mice 14 days after FA. (n=5-7) Scale bar: 50 µm. (B-C) Picosirius red staining of kidney sections from *Col1a2-Cre* and *Txndc5^{Endo-ckO}* mice (B) 10 days after UUO or (C) 14 days after FA. (n=5-6) Scale bar: 50 µm. (D-E) Picosirius red staining of kidney sections from *Txndc5^{fllox/fllox}*, *Txndc5^{Epi-ckO}* and *Txndc5^{Pod-ckO}* mice (D) 10 days after UUO or (E) 14 days after FA. (n=5-6) Scale bar: 50 µm. Data are representative of three or more independent experimental replicates. For all panels, data are presented as mean ± SEM. The statistical significance of differences among three or more groups was determined using one-way ANOVA, followed by Sidak's post hoc tests. *P<0.05, **P<0.01, ***P<0.001 by Sidak's multiple comparisons test.



Supplementary Figure 7. Deletion of *Txndc5* in kidney fibroblasts protects against TEC apoptosis in response to kidney injury. (A-B) TUNEL staining of kidney sections from (A) WT and *Txndc5*^{-/-} mice or (B) *Col1a2-Cre* and *Txndc5*^{fl/fl} mice 10 days after UUO. (n=3) Scale bar: 100 μ m. (C-D) Immunofluorescence staining of macrophage marker F4/80 (C, 5 days after UUO) and endothelial marker CD31 (D, 10 days after UUO) of kidney sections from WT and *Txndc5*^{-/-} mice. (n=3 for each group) Scale bar: 100 μ m. Data are representative of three or more independent experimental replicates. For all panels, data are presented as mean \pm SEM. The statistical significance of differences among three or more groups was determined using one-way ANOVA, followed by Sidak's post hoc tests. *P<0.05, **P<0.01, ***P<0.001 by Sidak's multiple comparisons test.

A



B

1	<i>Txndc5</i> 3VR1	5'- GGATGAGTAATGGAGTCGTGTGT-3'
2	<i>Txndc5</i> 3VF1	5'- GTAGCATAGCCACTATGTCACCA-3'
3	<i>Txndc5</i> 5VR1	5'- GTTGTACTTGTCTCCCAGGTCAT-3'
4	<i>Txndc5</i> 5VF1	5'- GGAGGAAGTGATGCCAAACTAGA-3'

C

Primer	PCR product size	Target site
3VF1+3VR1	409 bp (WT) 449 bp (LoxP knock-in)	3' LoxP site
5VF1+5VR1	447 bp (WT) 487 bp (LoxP knock-in)	5' LoxP site

Supplementary Figure 8. Generation of *Txndc5*^{fl/fl} mice using CRISPR/Cas9-based genome editing (A) Illustration of the experimental design to generate *Txndc5*^{fl/fl} mice using CRISPR/Cas9 genome editing. Arrows indicate the primers for genotyping and the orange line indicates the probe for Southern blotting. (B) List of primers for the genotyping of *Txndc5*^{fl/fl} mice. (C) The PCR product information used to identify 3' and 5' loxP knock-in sequences at the intended target site.